HDR image formation from CMOS coupled with MCP image intensifier

P. MIHAILOVIC[*], M. BARJAKTAROVIC, S. PETRICEVIC
School of Electrical Engineering, University of Belgrade, Bulevar kralja Aleksandra 73, Serbia

Images obtained from image intensifier (II) tubes offer good insight into objects illuminated at low light levels. Since the dynamic range of II is very high, it is possible to construct high dynamic range images using information on the II tube gain when the screen image is recorded using a CMOS sensor. This paper presents a method for creating the best array of images for high dynamic range (HDR) image formation. In this method the microchannel plate screen current is measured to detect sudden HDR image appearance. A night vision module microcontroller commands CMOS camera exposure times during the steep change of microchannel plate gain. Test results demonstrate good quality images in high contrast environments.

1. Introduction

Coupling of micro channel plate (MCP) based image intensifier screen with a CMOS camera produces a device that can be used in surveillance systems to enable the system to operate in extremely low levels of light. Most of the time this system operates in a dark environment and captures only low dynamic range (LDR) scenes. A problem occurs when the part of the imaged scenery becomes illuminated with high light levels in a short time interval. At an arbitrary moment the system can be exposed to artificial light that will leave some of the pixels saturated (for example, a car turning on lights in a dark parking lot or a person opening the door of a dark office). LDR scene swiftly becomes high dynamic range (HDR) and vice versa. In the case of surveillance systems key information can be lost. Although MCPs have adjustable gain this is not a solution to the problem since MCP gain is reduced according to total screen luminance and with some delay.

Capturing and displaying High-Dynamic-Range (HDR) scenes have been studied for some time with good results [1]. The Problem with LDR images in HDR scenes is usually solved by merging images captured with several exposure values. This procedure is called exposure bracketing. The basic idea is that different regions of the image need different integration intervals. Bracketing is usually achieved automatically by the camera, and this is standard for almost all smartphones.

Fig. 1(a) and Fig. 1(b) are presented to help illustrate the situation of an LDR scene swiftly becoming high dynamic range (HDR). In Fig. 1(a) one can see the interior of an office illuminated only by moonlight through a narrow window. Exposure time is fixed to $T_{emax} = 135$ ms. The picture in Fig. 1(b) appeared after a person opened the door. Bright light from a hallway saturates part of the pixels leaving the person unrecognizable.
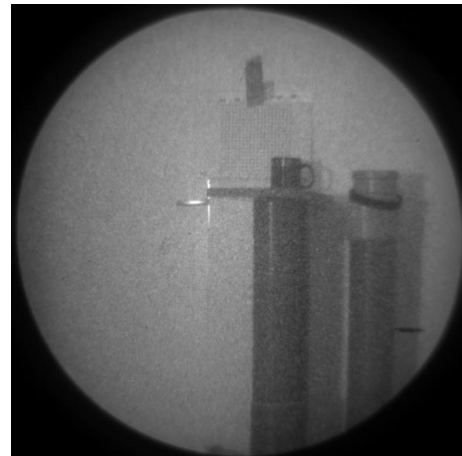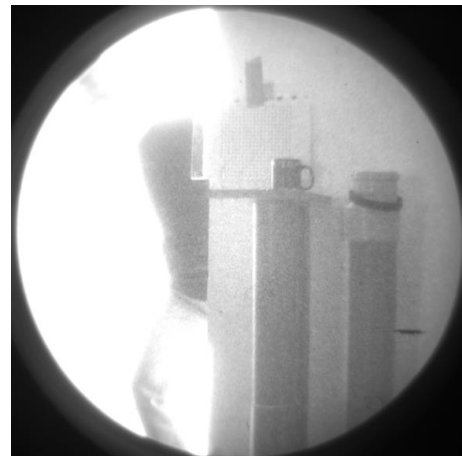

Fig. 1a. Dark scene

Fig. 1b. Illuminated scene

Electrically speaking, when a step change is applied to the MCP to control gain, the MCP voltages response behaves similarly to a first order system with the time constant τ_{MCP}. This causes screen luminance to react with some delay. During the matching of the power supply unit (PSU) with the image intensifier tube, the power supply is adjusted to provide exactly the required optical gain of the image intensifier. This means that, although the MCP voltage is varied when the cathode illumination varies, the screen luminance remains constant. The automatic brightness control in the power supply changes the MCP voltage so as to maintain screen luminance. This paper considers the described situation and proposes an algorithm for exposure time sequence and HDR image formation.

2. Image intensifier characteristics

A typical 3rd generation image intensifier unit is enclosed in a tubular body with the cathode opening and screen on the opposite flat sides. Power is provided by 2 copper plated contacts on the sides. There are no additional adjustments, since the II power supply was matched to the II tube in the factory to provide the required optical gain in low light conditions. Matching requirements are well known and standardized [2] leading to typical luminous gains of 50000 for low light levels of cathode illumination, but since cathode illumination can range from 10^{-5} lx up to 200 lx, the PSU must provide gain reduction in order to maintain constant screen brightness. This function is known as automatic brightness control (ABC) that operates by reducing the MCP voltage in order to reduce the gain when the cathode illumination increases. For practical purposes II operation zones are divided into: low light level, ABC range and high light level. Low light level operation occurs when cathode illumination is below 10^{-3} lx without gain reduction and screen brightness varies with cathode illumination. In the ABC zone (above 10^{-3} lx) MCP voltage is varied in order to maintain constant screen brightness by measuring the screen current as an input to the control loop. The third operational zone, high light level mode, is generally taken to be above 10 lx and modern II reduce the tube gain by

gating the cathode voltage with pulse-width modulation (PWM). Loss of resolution in third operational zone has been to greater extent resolved in 3rd generation II using PSU with autogated mode of operation.

This ABC loop exhibits a certain delay since screen brightness takes some time to settle after cathode illumination change, depending on the range of change and on the operational mode of the tube. For reasons involving screen current measurement at the screen multiplier return node the screen current error integrator is designed with a time constant in the range of 40 ms. This ensures low noise in the integrator output voltage that controls the MCP voltage and stability of the loop. Depending on the range of change of cathode illumination, the PSU will drive the MCP into a new steady state, causing the MCP voltage to change in a time range of up to 200 ms. A typical screen brightness for a modern 3rd generation II exhibits transition waveform as seen in Fig. 2, obtained by monitoring the screen brightness when the cathode illumination changed from 10^{-4} lx to 10^{-1} lx. The emphasized overshoot is present at the transition beginning caused by maximum gain of the MCP due to high applied voltage. Once the screen current rises to a level corresponding to the screen brightness the ABC begins to regulate by dropping the MCP voltage (some screen voltage drop is also present due to high screen multiplier output impedance that also causes brightness drop). The MCP voltage continually drops in the middle part of the waveform in the form corresponding to exponential discharging of the 1st order RC circuit. This is in fact caused by passive MCP voltage discharge of the MCP capacitance with its resistance since compact PSU units are unable to discharge MCP capacitance actively due to the size limitations of the PSU housing preventing use of high voltage transistors. A typical MCP exhibits around 200 pF of capacitance and 200 MΩ resistance [3] creating an eigen time constant of $\tau_{MCP} = 40$ ms so that the 5τ point is reached at 200 ms, matching the oscilloscope recording nicely. Some undershoot is visible following RC discharge caused by screen multiplier charging causing incorrect screen current measurement and finally the waveform settles to steady state.
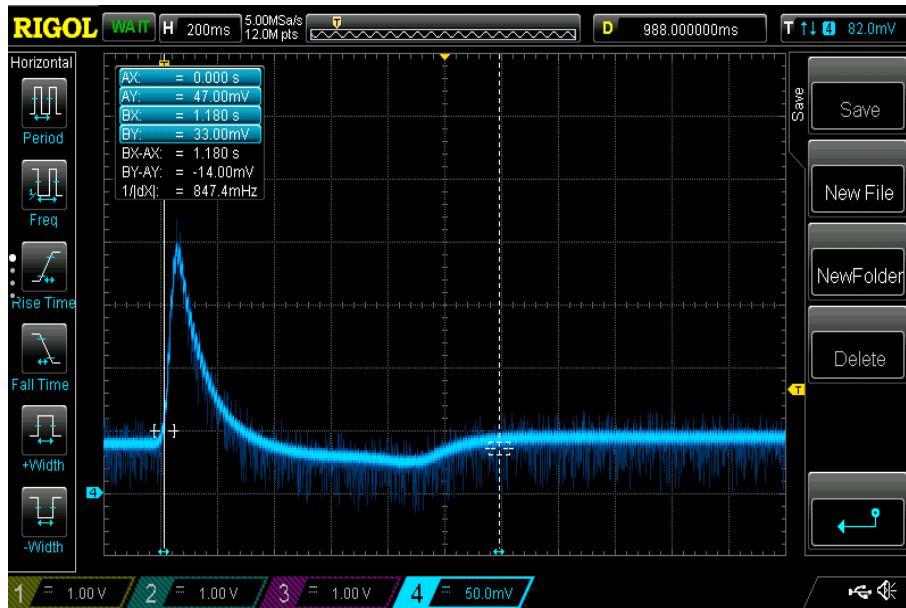
Fig. 2. Typical screen brightness variation during step change in cathode illumination (color online)

Since the MCP voltage and thus gain is varied during the transition period, MCP gain and thus screen brightness during transition must be known in order to obtain an HDR image. MCP gain has been recorded and is presented in Fig. 3.

MCP gain in low light and ABC modes varies from 10000 to 1 (4 decades of dynamic range which shall be denoted as R below) giving the possibility of a very high dynamic range to the HDR image after processing. This range is indeed useful, since even if a very small part of the II photocathode is subjected to high illumination levels, large screen current results, dropping the MCP gain all the way down the gain-voltage curve.
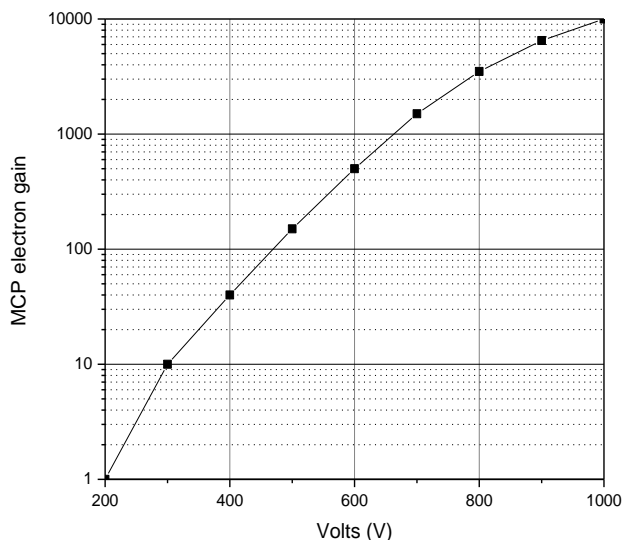

Fig. 3. MCP gain versus applied voltage

The most common II configuration uses a P43 phosphorus screen for image projection. When coupled to a CMOS camera this type of phosphorus screen was found to exhibit good linearity [4] with a decay time below 2 ms. In practical terms screen characteristics do not affect the image creation algorithm since the phosphorus decay time is shorter than the MCP reaction time. The signal to noise ratio (SNR) of the II also affects the image quality. For a modern II tube an SNR of 24 is achievable [5] but this still mandates some noise reduction in the algorithm to achieve good quality images.

3. Algorithm design

The standard procedure of continuously taking a sequence of pictures with exposure times from $T_{emin}=T_{e1}$ to $T_{emax} = T_{eN}$ is suboptimal here for two reasons. First, all the pictures taken in a dark environment with exposure times different from T_{emax} will be underexposed and therefore useless. The second reason originates from a scenario where a bright object emerges at the end of the minimal exposure time T_{e1}. In this instance the MCP gain begins to fall while exposure times increase, partially canceling each other out and reducing the information content.

Instead of this, the camera is driven by the microcontroller unit (MCU) to take the pictures with maximal exposure times, adjusted to expected low illumination, until a new sequence of MCU control signals starts. The MCU inside the PSU (8 bit PIC) handles the measurement and control function. MCP voltage and screen current are continually monitored using the ADC in the MCU, and the MCP drive is varied in order to maintain constant screen current. Depending on the screen current change the MCP voltage is varied in reverse direction in

order to return the screen current to the set point (usually more than 100 nA) thus maintaining the screen brightness. Fig. 4 presents time diagrams of MCP voltage (red), MCP drive (white dots), screen current (yellow) and some additional internal parameters (cathode clamp voltage and transformer duty cycles) of the MCU operations.
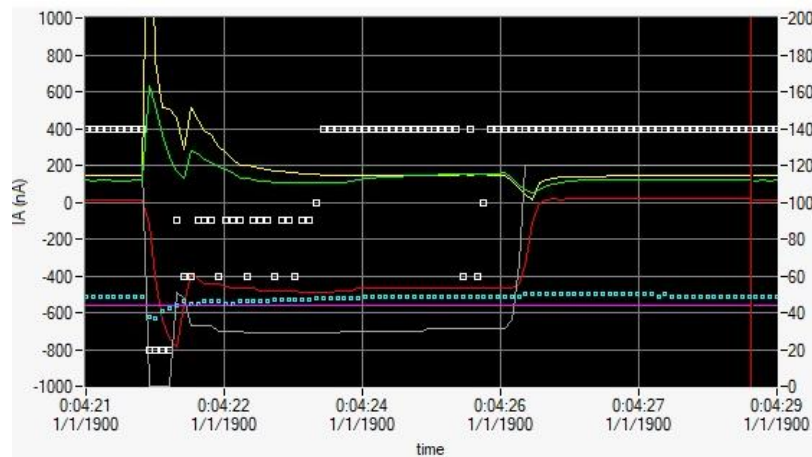

Fig. 4. Behavior of image intensifier during change of cathode illumination from 0.2 lx to 10 lx (color online)

When the Gen3 II cathode is illuminated with high light levels, the power supply reduces MCP voltage from the kV level to several hundred volts. The action is caused by the steep rise in screen current from around 100 nA up to several μA. Such high screen current levels are caused by high MCP gain before voltage reduction takes places, and have been used as a trigger that initiates a new sequence of control signals from MCU to camera.

As can be seen in Fig. 4 when the II is illuminated with 10 lx the screen current (yellow line, left axis nA) reaches above 1 μA level and the MCP voltage (red line, right axis scale is x10 in volts) drops from above 1 kV to 550 V, stabilizing to set level after about 2 seconds. This particular case is for a fully autogated PSU where bright screen protection (BSP) is provided by lowering the duty cycle of the cathode voltage. This means that the cathode voltage is not reduced, as is the case with non-gated PSU, and the resolution is maintained at above 50 lp/mm even in high light conditions. This is a necessary requirement for the HDR algorithm to work properly. The second screen current spike is created by a "rebound" of MCP voltage when the gating begins, since gating reduces cathode current and thus the MCP recharges somewhat (600V). The trigger is taken at the point where screen current exhibits steep rise (1st derivative is calculated). The threshold value can be adjusted according to surveillance system type and expected situations.

Following this internal MCU trigger, the MCU generates a series of control signals forwarded to camera's input on the 6-pin port. Camera control signals are slaved to the PSU gating frequency of 100 Hz in order to eliminate camera flicker. The pulse sequence contains 20 pulses for a total of 200 ms length thus corresponding to the $5\tau_{MCP}$ condition. As the sequence progresses pulses increase in length in order to increase exposure time. Rising edge of each pulse starts camera's exposure which ends with falling edge of each pulse. In the opposite case when cathode illumination changes from high to lower levels, the trigger detection algorithm and pulse train behave in the opposite manner.

Under normal operational conditions (low light illumination) the screen current noise level is around few nA (almost invisible in Fig. 4 with stable illumination) so the noise does not affect the trigger generation due to the good signal/noise ratio of Gen3 tubes.

We consider only the critical period of time during which MCP gain is changing. The decision about exposure times after this period should involve image processing but after the steady state appears there is enough time for that.

The control sequence commands the camera to take pictures with exposure times (T_{e1}, T_{eN}, T_{e1}, T_{eN-1}, T_{e1},…, T_{e2}); where $T_{eN} > T_{eN-1}$. The last picture taken before the control sequence appeared, with the period T_{e0}, which we do not influence, but which is measured and known, should also be used for HDR picture formation. The sequence starts with T_{e1} in order to swiftly obtain information about highly illuminated part of the picture. The second term should produce sufficient information from the least illuminated part since the MCP gain is still high and the exposure time is long. The even members of the exposure times sequence are monotonically decreasing having the same effect on pixel value change as the MCP gain drop, giving us the maximal amount of information for total sequence time.

4. Image processing

In this research we used a Basler industrial camera acA2440-75um. This camera model has a CMOS type sensor with a resolution of 5 MP, a global shutter and USB 3.0 connection to a PC or some embedded vision computer like Jetson Nano by NVIDIA.

After getting the image sequence, the problem is how to encode and merge images, because all are in range of 0–255 (only integers) and we must accommodate full intensity range of the scene. To deal with this problem, algorithms for HDR image formation use a well-established procedure and most implementation are based on work by Devebec and Malik [6], and we also used it in our research. There are also some newer methods for HDR imaging, a number of the more up-to-date are based on deep learning techniques [7-9]. But they have long inference times and for some there is a lack of their implementation, or only Python code exists. In contrast, Devebec's algorithm is implemented in OpenCV library with C++ code and it is optimized for real-time execution not only for PC but for microcontrollers too. Also, multi-exposure merging algorithm is utilized for many implementations of HDR imaging in mobile devices [19], because it does not require special HDR sensors with advanced architecture which are novel [20] but expensive chips.

Devebec's algorithm starts with an estimation of the Camera Response Function (CRF). CRF is a function that connects scene irradiance and the digital values in the image taking exposure value into account. Manufacturers of digital cameras don't provide CRFs for their models and consider CRF as proprietary information.

For each camera CRF can be estimated by images of the same scene with HDR characteristics using several different exposure values. In every image j we take the digital value Z at the spatial location i. We denote this digital value with Z_{ij}. If Δt_j is the exposure interval for j image, and E_i is irradiance at spatial location i, Camera Response Function f connects all these three values as in equation (1).

$$Z_{ij} = f\left(E_i \Delta t_j\right) \qquad (1)$$

To estimate the CRF of Basler camera acA2440-75um we used the test image shown in Fig. 5(a). Using the function provided by OpenCV, we get the CRF for this camera model, Fig. 5(b):
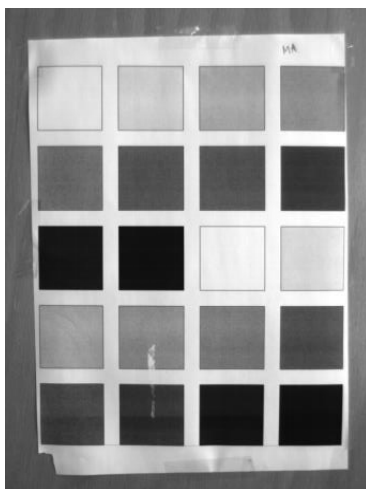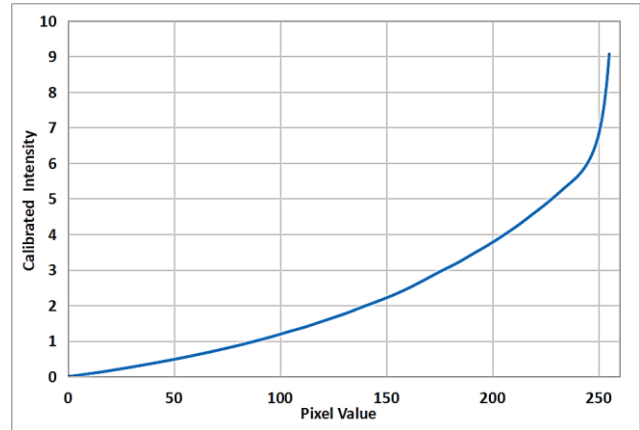

Fig. 5b. CRF of Basler camera acA2440-75um

The Night Vision Module (NVM), shown in the Fig. 6, as a whole system has different CRF from camera alone.
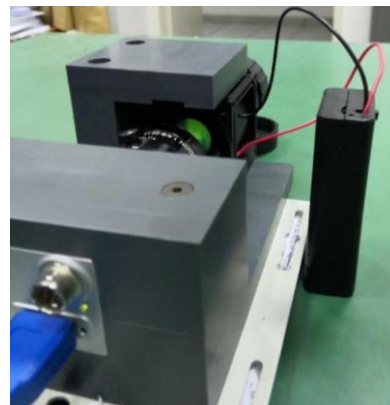

Fig. 6. Night Vision Module (color online)

The standard response curve considers the whole visible spectral range, introducing the integration effect, but II has a display which radiates only in a narrow part of the green wavelengths. Test image for obtaining the CRF of the Night Vision Module is shown in Fig. 7(a) and the CRF in Fig. 7(b).
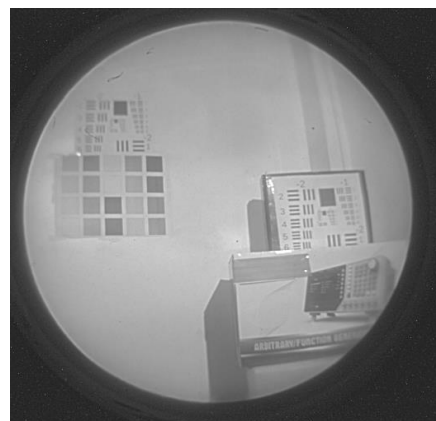

Fig. 5a. Test Image for finding CRF
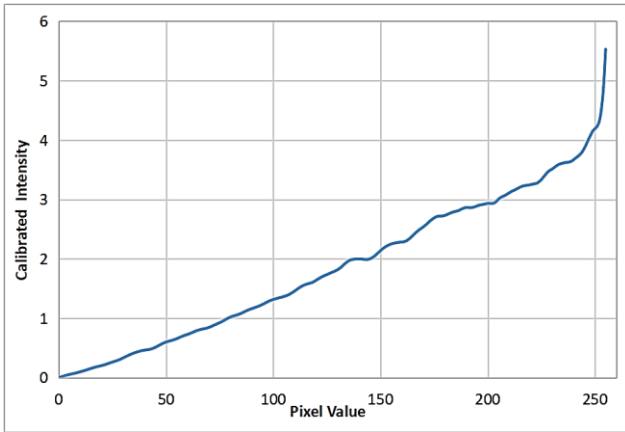

Fig. 7a. Test Image for finding CRF

Fig. 7b. CRF of Night Vision Module

MCP gain, $G(t)$, is time dependent and pixel illumination also depends on phosphorescence. If the artificial light is time varying, per pixel irradiance, $E_i(t)$, is time dependent too. Pixel values Z_{ij} can be calculated from equation (2)

$$Z_{ij} = f_{NVM}\left(\int_0^{Tej} G(t)E_i(t)dt\right) \quad (2)$$

where f_{NVM} is the response function, as before, but now for NVM. This means that it is not possible to obtain CRF and use it for generating HDR images onwards by the procedure described by Debravec and Malik directly. Fortunately, we monitored MCP gain $G(t)$ and modified the procedure slightly. The CRF of the NVM has to be predetermined on steady scenes and we did this with 10 images. We used a similar test image as before, shown in Fig. 6(a), repeat CRF calibration process and get new CRF, Fig 6(b). Scene are arranged in such a way that gain was G=500 which is at middle of the MCP voltage range. MCP is a linear device in respect to irradiance, and for true irradiance (up to a scale factor, which has no influence on further image processing) we need to divide the irradiance obtained by the Debravec and Malik algorithm by G=500. For every image acquired at time instance t we know the exposure interval $\Delta t(t)$ and MCP gain $G(t)$. During $\Delta t(t)$ the lighting was kept constant keeping the MCP gain $G(t)$ approximately constant as well. Using the response function for NVM we obtain pixel irradiance $E(t)$ as calculated by equation (3).

$$ln[E_i(t)] = lnf_{NVM}^{-1}[Z_i(t)] - ln[\Delta t(t)] - ln[G(t)] \quad (3)$$

Equation (3) is to find irradiance from one image at the position i. For a sequence of P images, the equation (4) can be derived.

$$lnE_i = \frac{\sum_{j=1}^{P}\omega(z_{ij})[lnf_{NVM}^{-1}(z_{ij}) - ln\Delta t_j - lnG_j]}{\sum_{j=1}^{P}\omega(z_{ij})} \quad (4)$$

where w(Z) is a weighting function, which penalizes values which are not in the middle of the brightness range as in equation (5).

$$\omega(z) = \begin{cases} z - Z_{min} \; for \; z \leq \frac{1}{2}(Z_{min} + Z_{min}) \\ Z_{max} - z \; for \; z > \frac{1}{2}(Z_{min} + Z_{min}) \end{cases} \quad (5)$$

After we obtain an HDR image, the next step is to prepare it for display on a standard screen. For that reason, the wide dynamic range needs to be compressed to the 0–255 range of grayscale format. This process is called Tone Mapping (TM) and it can be done in many ways. TM is an active research field many algorithms have been published and it is not clear which is optimal. Ranking depends on application and testing criteria [10]. In the OpenCV library four Tone Mapping Operators (TMO) have been implemented [11-14]. OpenCV library is highly optimized and application developed using OpenCV can execute on all major platforms.

We measured the execution speed for all of them and found that Mantiuk is more than 10 times slower than Drago and Reinhard, which have similar execution time and they are about 2.5 times faster than Durand's method. Although, by tuning parameters of all four algorithms we got almost the same subjective results, we chose Reinhard method for our algorithms because it was ranked among the best in several research [9], [15-16] and it can be run in local or global mode. Global TMOs use same mapping for all pixels in image and local ones take into account spatial information. Reinhard's algorithm can be described using equations (6),

$$I_a(x,y) = a * HDR(x,y) + (1-a)HDR_{avg}$$

$$LDR(x,y) = \frac{HDR(x,y)}{HDR(x,y) + (f*I_a(x,y))^m} \quad (6)$$

$$LDR(x,y) = 255 * \frac{LDR(x,y) - LDR_{min}}{LDR_{max} - LDR_{min}}$$

where, HDR_{avg} is the average intensity in an HDR image and a, m and f are user specified parameters: adaptation, contrast and overall intensity, respectively. This gives possibility to optimize NVM to expected contest in the particular surveillance task depending on which characteristics of the scene should be enhanced, global or local ones. This, together with real time performance makes Reinhard's operator best choice among implemented ones in OpenCV.
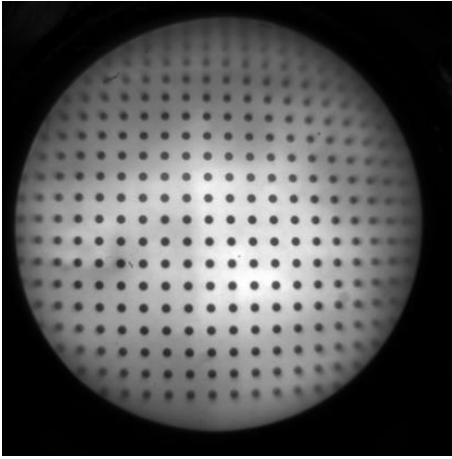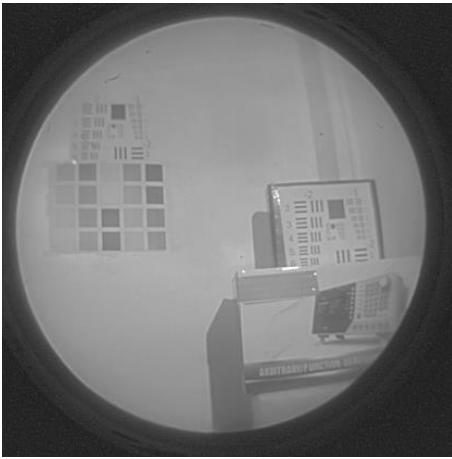
Fig. 8a. Rectification map
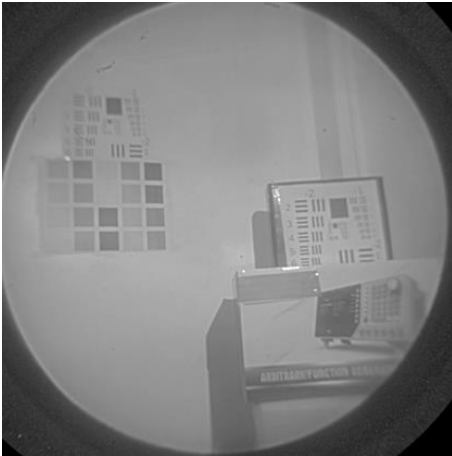

Fig. 8b. Image before undistortion


Fig. 8c. Image after undistortion

Also, the lens of the MCP module introduce some barrel distortion, which can be compensated for using a rectifying map, Fig. 8(a). For undistortion we used the standard procedure implemented in the OpenCV library [17]. Images before and after undistorting are shown in Fig. 8(b) and Fig. 8(c) respectively.

5. Results

The algorithm is demonstrated on the same situation as described in the introduction (a person opening the door of a dark office). The number of pictures in the sequence is $2N$-2. Since we included the last picture with T_{e0} exposure time in the HDR picture formation there are $2N$-1 pictures for image formation. If the MCP dynamic range is R and the camera dynamic range is F the number of exposure times $N_{MAX} = \left[\frac{R}{F}\right]$ guaranties that there will be no overexposed pixel. Yet, the higher the N the more ghosting there will be in the HDR picture of the dynamic scene. Therefore, N is the compromise between information gain and frame rate. In a real situation R can possibly occur only at the first moment of HDR scene appearance when the MCP gain is maximal. Since MCP gain is variable it decreases and draws saturated phosphorus out of saturation. At the same time "dark" pixels become more illuminated due to reflected and scattered light (laser illumination excluded). Since MCP channels are equal, the gain is the same for every pixel and cancels out leaving the dynamic range of image illuminating CMOS the same as the dynamic range of the scene itself. If we denote dynamic range of the scene with D then sufficient $N < N_{MAX}$ is $N = \left[\frac{D}{F}\right]$. Another parameter that influences N is the MCP time constant τ_{MCP}, since sequence duration should last approximately same as $5\tau_{MCP}$. Thus, N depends on the dynamic range of the scene (often unknown), dynamic range of the camera and MCP time constant. For our MCP $\tau_{MCP} = 40$ ms and $T_{emax} = 135$ ms. We chose $N = 3$ with $T_{e1} = 10$ ms, $T_{e2} = 60$ ms, $T_{e3} = 120$ ms. This gives us a sequence duration of $T = T_{e1} + T_{e3} + T_{e1} + T_{e2} = 200$ ms $= 5\tau_{MCP}$ and 5 pictures for HDR image formation: $P0(T_{e0})$, $P1(T_{e1})$, $P2(T_{e3})$, $P3(T_{e1})$, $P4(T_{e2})$ displayed in Fig. 9. together with picture P-$1(T_{emax})$ taken just before the door was opened. Please note that $P1(T_{e1})$ differs from $P3(T_{e1})$ since MCP gain is changed.
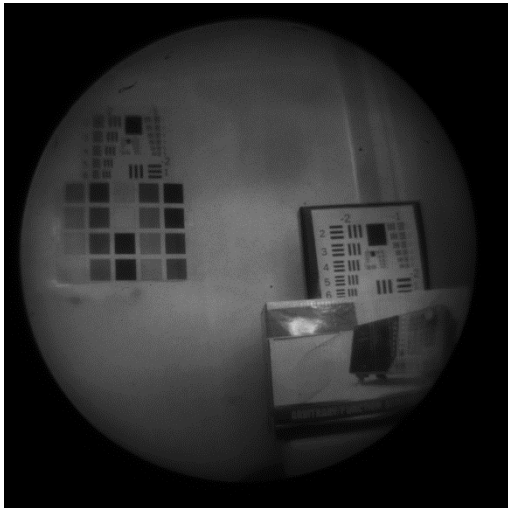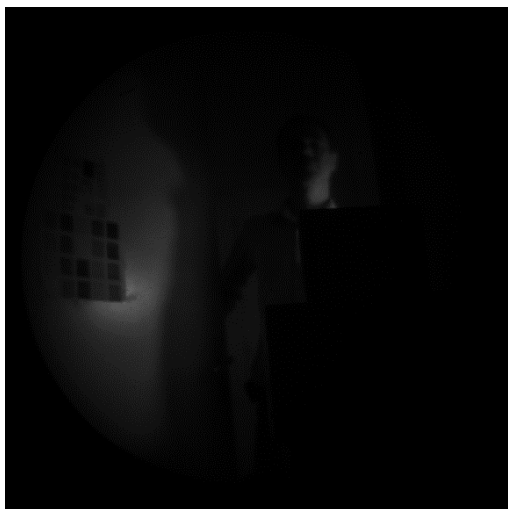
P-1(Temax)
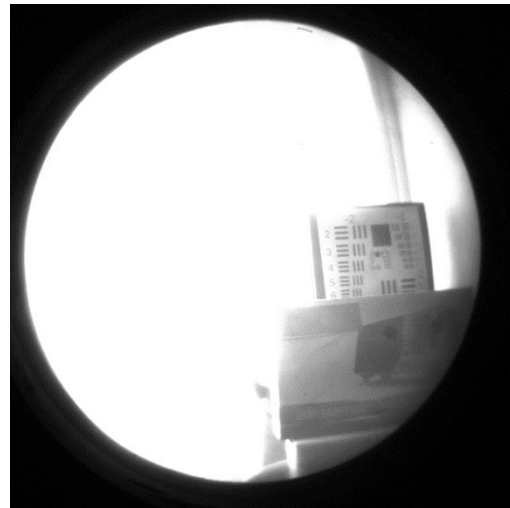
P0(Te0)

P1(Te1)

P2(Te3)

P3(Te1)

P4(Te2)

Fig. 9. Array of unprocessed images with exposure times in brackets

The tone mapped HDR image is shown in the Fig. 10, which was obtained using the algorithm described in the previous section with an added unsharp mask [18] to emphasize edges and make the image more pleasing to the observer.

Fig. 10. Final image

6. Discussion

Although we considered only one possible scenario of sudden HDR image appearance we think that this paper presents guidelines for resolving similar situations when surveillance camera has II tube in front of it. The most critical period is during the steep change of MCP gain. The screen current of the MCP is the variable that should be monitored for fastest reaction time. The CRF of the whole system has to be predetermined. For this one needs to know and control MCP gain in the function of voltage. The time constant of the MCP has to be measured. Having done this, we devised the algorithm for a dark office surveillance. Beside expected situation, the algorithm depends on the MCP time constant and the dynamic range of the camera. After the HDR image formation and image processing we got the image that preserved information about both, the dark and the bright parts of the scene in the critical transition period.

References

[1] A. Nayana, A. K. Johnson, Int. J. of Im. Proc. **9**, 198 (2015).

[2] H. K. K. Photonics, "Image Intensifiers", Hamamatsu, p. 8 (2020).

[3] J. Ladislas Wiza, Nucl. Instrum. Methods **162**, 587 (1979).

[4] A. R. Faruqi, G. C. Tyrell, Ultramicroscopy **76**(1–2), 69 (1999).

[5] S. A. Baker, N. S. P. King, W. Lewis, S. S. Lutz, D. V. Morgan, T. Schaefer, M. D. Wilke, "High-Speed Imaging and Sequence Analysis II", A. M. Frank and J. S. Walton, eds. (SPIE, 2000), 39 (2000).

[6] P. E. Debevec, J. Malik, Proceedings of the 24th Annual Conference on Computer Graphics and Interactive Techniques, SIGGRAPH, 369 (1997).

[7] N. K. Kalantari, R. Ramamoorthi, ACM Trans. Graph. **36**(4), 12 (2017).

[8] G. Eilertsen, J. Kronander, G. Denes, R. K. Mantiuk, J. Unger, ACM Trans. Graph. **36**(6), 15 (2017).

[9] D. Marnerides, T. Bashford-Rogers, J. Hatchett, K. Debattista, Comput. Graph. Forum **37**(2), 37 (2018).

[10] X. Cerdá-Company, C. A. Párraga, X. Otazu, J. Opt. Soc. Am. A **35**(4), 626 (2016).

[11] F. Drago, K. Myszkowski, T. Annen, N. Chiba, Computer Graphics Forum, Blackwell Publishing Ltd, **22**(3), 419 (2003).

[12] F. Durand, J. Dorsey, ACM Trans. Graph. **21**(3), 257 (2002).

[13] E. Reinhard, M. Stark, P. Shirley, J. Ferwerda, ACM Trans. Graph. **21**(3), 267 (2002).

[14] R. Mantiuk, K. Myszkowski, H. P. Seidel, ACM Trans. Appl. Percept. **3**(3), 286 (2006).

[15] J. Kuang, H. Yamaguchi, G. Johnson, M. Fairchild, "Testing HDR image rendering algorithms," Present. other Scholarsh. (2004).

[16] M. Čadík, M. Wimmer, L. Neumann, A. Artusi, Comput. Graph. **32**(3), 330 (2008).

[17] A. Kaehler, G. Bradski, "Learning OpenCV", O'Reilly Media, Inc. 580 (2016).

[18] R. C. R. E. W. Gonzalez, Digital Image Processing (3rd Edition), (2008).

[19] R. Mantiuk, M. Cichowicz, M. Smyk, Implementation of HDR Photographic Pipeline in Mobile Devices, Lecture Notes in Computer Science **7324**. Springer, Berlin, Heidelberg. https://doi.org/10.1007/978-3-642-31295-3_43

[20] OmniVision, HDR Technology, https://www.ovt.com/hdr, visited 23.10.2020.

_____
[*]Corresponding author: slobodan@etf.rs